

## Research Article

# ASKAP EMU radio detection of the reflection Nebula VdB-80 in the Monoceros crossbones filamentary structure

Aaron Bradley<sup>1</sup>, Zachary Smeaton<sup>1</sup>, Nicholas Tothill<sup>1</sup>, Miroslav D. Filipović<sup>1</sup>, Werner Becker<sup>2,3</sup>, Andrew Hopkins<sup>4</sup>,  
Bärbel Silvia Koribalski<sup>1,5</sup>, Sanja Lazarević<sup>1,5,6</sup>, Denis Leahy<sup>7</sup>, Gavin Rowell<sup>8</sup>, Velibor Velović<sup>1</sup> and Dejan Urošević<sup>9</sup>

<sup>1</sup>Western Sydney University, Penrith South DC, NSW, Australia, <sup>2</sup>Max-Planck Institut für extraterrestrische Physik, Garching, Germany, <sup>3</sup>Max-Planck-Institut für Radioastronomie, Bonn, Germany, <sup>4</sup>School of Mathematical and Physical Sciences, Macquarie University, Sydney, NSW, Australia, <sup>5</sup>Australia Telescope National Facility, CSIRO, Space and Astronomy, Epping, NSW, Australia, <sup>6</sup>Astronomical Observatory, Belgrade, Serbia, <sup>7</sup>Department of Physics and Astronomy, University of Calgary, Calgary, AB, Canada, <sup>8</sup>School of Physics, Chemistry and Earth Sciences, The University of Adelaide, Adelaide, Australia and <sup>9</sup>Department of Astronomy, Faculty of Mathematics, University of Belgrade, Belgrade, Serbia

### Abstract

We present a new radio detection from the Australian Square Kilometre Array Pathfinder Evolutionary Map of the Universe (EMU) survey associated with the Reflection Nebula (RN) VdB-80. The radio detection is determined to be a previously unidentified HII region, now named *Lagotis*. The RN is located towards Monoceros, centred in the molecular cloud feature known as the ‘Crossbones’. The 944 MHz EMU image shows a roughly semicircular HII region with an integrated flux density of  $30.2 \pm 0.3$  mJy. The HII region is also seen at 1.4 GHz by NRAO VLA Sky Survey (NVSS), yielding an estimated spectral index of  $0.65 \pm 0.51$ , consistent with thermal radio emission. *Gaia* Data Release 3 (DR3) and Two Micron All Sky Survey (2MASS) data give a distance to the stars associated with the HII region of  $\sim 960$  pc. This implies a size of  $0.76 \times 0.68 (\pm 0.09)$  pc for the HII region. We derive an HII region electron density of the bright radio feature to be  $26 \text{ cm}^{-3}$ , requiring a Lyman-alpha photon flux of  $10^{45.6} \text{ s}^{-1}$ , which is consistent with the expected Lyman flux of HD 46060, the B2 II type star which is the likely ionising star of the region. The derived distance to this region implies that the Crossbones feature is a superposition of two filamentary clouds, with *Lagotis* embedded in the far cloud.

**Keywords:** ISM: nebulae; ISM: HII region; ISM: clouds; ISM: molecules; proper motions; stars: distances

(Received 18 December 2024; revised 31 January 2025; accepted 7 February 2025)

## 1. Introduction

Reflection Nebulae (RNe) are diffuse clouds of gas and dust typically associated with star-forming regions. These RNe are illuminated by young stars and may be accompanied by emission nebulae (Mueller & Graham 2000; Eiermann et al. 2024). These nebulae are prominent in visible wavelengths, but the visible emission of a RN may be obstructed by dark molecular gas and dust, so the full extent is often better seen in near-infrared (Whitcomb et al. 1981) and far-infrared (Sellgren 1984) wavelengths.

VdB-80 (also known as [RK68]-59), is a known Galactic RN in the constellation Monoceros, below the Galactic plane at  $l = 219^\circ 26'$ ,  $b = -8^\circ 93'$  (RA(J2000)  $\sim 06^{\text{h}} 31^{\text{m}}$ , DEC(J2000)  $\sim -9^\circ 39'$ , van den Bergh 1966; Rozhkovskij & Kurchakov 1968; Magakian 2003).

HII regions are typically associated with sites of early star formation or young stellar clusters embedded in molecular clouds and are comprised of ionised hydrogen (Dyson & Williams 1997). Ahumada et al. (2001) did not see any signs of an HII region

towards VdB-80 in their optical spectra. Nonetheless, we identify radio emission detected by Australian Square Kilometre Array Pathfinder (ASKAP) as an HII region that we name ‘*Lagotis*’,<sup>a</sup> associated with a stellar cluster in the ‘Crossbones’ molecular cloud, and it is proposed that the star HD 46060 is the centre of both RN and HII region.

The Crossbones is a filamentary cloud structure located within the Mon R2 complex, first characterised by Maddalena et al. (1986), potentially related to the Orion-Eridanus superbubble (Lee & Chen 2009). This ‘X’ shaped structure is an active star-forming region, with VdB-80 bordering the cloud near to its centre. The structure is most clear in maps of the ( $J = 1-0$ ) rotational transition of  $^{12}\text{CO}$  (Dame et al. 1987; Ghosh, Remazeilles, & Delabrouille 2024).

The ASKAP (Hotan et al. 2021) Evolutionary Map of the Universe (EMU) (Norris et al. 2011, 2021, Hopkins et al., PASA, submitted.) survey has provided new radio-continuum observations of this region with improved sensitivity compared to any previous radio-continuum surveys. Higher sensitivity has allowed for the first reliable detection of radio-continuum emission toward VdB-80. This new radio detection allows us to estimate properties of the RN that confirm the presence of a HII region, as well as confirming HD 46060’s role as the star responsible for creating both features.

<sup>a</sup>Named after the Australian Greater Bilby (see Section 3.4).

**Corresponding author:** Aaron Bradley; Email: 20295208@student.westernsydney.edu.au.

**Cite this article:** Bradley A, Smeaton Z, Tothill N, Filipović MD, Becker W, Hopkins A, Koribalski BS, Lazarević S, Leahy D, Rowell G, Velović V and Urošević D. (2025) ASKAP EMU radio detection of the reflection Nebula VdB-80 in the Monoceros crossbones filamentary structure. *Publications of the Astronomical Society of Australia* 42, e032, 1–8. <https://doi.org/10.1017/pasa.2025.15>

This radio detection demonstrates the ability of the newest generation of radio surveys, such as EMU, to detect new low surface-brightness emission. This has been demonstrated in several new discoveries, such as supernova remnants G181.1–9.5 (Kothes et al. 2017), J0624–6948 (Filipović et al. 2022), G288.8–6.3 (Ancora; Filipović et al. 2023; Burger-Scheidlin et al. 2024), G121.1–1.9 (Khabibullin et al. 2023), G308.7+1.4 (Raspberry; Lazarević et al. 2024a), G312.6+ 2.8 (Unicycle; Smeaton et al. 2024), and a pulsar wind nebula (Potoroo; Lazarević et al. 2024b).

The paper is structured as follows: Section 2 outlines the data used, including radio, optical, and infrared data, both new and archival. Section 3 provides analysis and interpretation of Lagotis, this includes distance, size, emission properties and the context of the RN within the Crossbones filaments. Section 4 provides a brief summary of our results and interpretation of Lagotis.

## 2. Data

### 2.1 Radio observations

#### 2.1.1 The Australian Square Kilometre Array Pathfinder

The radio emission associated with VdB-80 was discovered in the ASKAP EMU (AS201) survey. Lagotis appears in two separate EMU observations: Scheduling Block SB59692 observed tile EMU\_0626 – 09A on 2024 March 02, and SB61077 observed tile EMU\_0626 – 09B on 2024 April 13. Both observations were taken at 943.5 MHz with a bandwidth of 288 MHz. The data were reduced using the standard ASKAP pipeline, ASKAPSoft, using multi-frequency synthesis imaging, multi-scale cleaning, self-calibration and convolution to a common beam size (Guzman et al. 2019).

We merged the two images using Multichannel image reconstruction, image analysis and display (MIRIAD) (Sault, Teuben, & Wright 1995) task IMCOMB. This merges the images together while applying weighting in the overlapped region to minimise rms noise. SB59692 had significantly more interference from a nearby bright star, and so the weighting ratio of 1:1.5, for SB59692:SB61077, was used to produce the best image. The resulting Stokes *I* image (Fig. 1) has a restored beam size of  $15 \times 15''$  and a local rms noise of  $\sim 20 \mu\text{Jy beam}^{-1}$ . There is no corresponding Stokes *V* emission.

#### 2.1.2 NRAO VLA Sky Survey

The NRAO VLA Sky Survey (NVSS) covers the entire sky north of  $-40^\circ$  (Condon et al. 1998), at 1.4 GHz in the radio continuum, with bandwidth 50 MHz. The Lagotis HII region is also present in this survey, which is used in Section 3.1 to obtain characteristics of the RN in radio wavelengths. The NVSS image used has a resolution of  $45'' \times 45''$  and a measured local rms noise of  $\sim 40 \mu\text{Jy beam}^{-1}$ .

#### 2.1.3 CO data

The Crossbones cloud was first observed by Maddalena et al. (1986) as part of the Columbia CO survey of the galaxy (Dame et al. 1987). Newer  $^{12}\text{CO}$  ( $J = 1 \rightarrow 0$ ) maps of the Galaxy have been derived from the broadband millimetre-wave maps obtained by the *Planck* satellite (Ghosh et al. 2024).

### 2.2 Optical observations

van den Bergh (1966) identified HD 46060 as the illuminating star of the RN, noting that it is ‘in a small compact clustering which includes BD  $-9^\circ 1497$ .’ Orellana et al. (2015) used the UCAC4 astrometric catalogue to identify 8 cluster members of the 23 proposed by Bonatto & Bica (2009).

#### 2.2.1 Gaia

*Gaia* data for 5 stars that appear to lie within the radio-continuum emission were taken from the *Gaia* Data Release 3 (DR3) (*Gaia* Collaboration et al. 2016, 2023) catalogue. These values, as well as derived distances, are reported in Table 1. Three of these stars are also listed by Orellana et al. (2015); the proper motions are fairly similar, except for UCAC4 402-013691 – Orellana et al. do not consider it to be a cluster member, but the *Gaia* proper motion (PM) measurement are much closer to the cluster average.

### 2.3 Infrared observations

#### 2.3.1 Two Micron All Sky Survey

Data were collected from Two Micron All Sky Survey (2MASS) (Skrutskie et al. 2006) and used in Section 3.2 to determine accurate distance estimates to the VdB-80, as well as confirming the distance association to the Lagotis HII region. The 2MASS All Sky Catalogue of point sources provides the magnitudes of the RN associated stars in the J, H and  $K_s$  (1.25, 1.65, and  $2.17 \mu\text{m}$ ) infrared bands. To verify the association of the RN and the HII region, these magnitudes, as well as a 2MASS J–H/H– $K_s$  extinction map from Froebrich et al. (2007), were used to determine stellar position and dust extinction values.

#### 2.3.2 Wide-Field Infrared Survey Explorer

The Wide-Field Infrared Survey Explorer (WISE) is an all-sky survey in near- and mid-infrared (Wright et al. 2010). Observations were taken in four bands, W1, W2, W3, and W4 with wavelengths 3.4, 4.6, 12, and  $22 \mu\text{m}$ . The W3 and W4 bands are used with EMU data (Fig. 2) to trace the mid-infrared emitting gas and dust that shows the full extent of the RN (Filipović & Tothill 2021a) at wavelengths other than optical.

#### 2.3.3 AKARI

The *AKARI* far-infrared All-Sky Survey (Doi et al. 2015) comprises four far-infrared bands (65, 90, 140, and  $160 \mu\text{m}$ ). *AKARI* data show the gas and dust shroud surrounding the Lagotis HII region and VdB-80 (Fig. 3) and are used in conjunction with optical and radio images to create an RGB composite (Fig. 4). *AKARI* survey data are useful for mapping the local area surrounding VdB-80, as well as the broader context of the Crossbones filaments.

## 3. Results and discussion

### 3.1 VdB-80 radio-continuum association

Lagotis, the VdB-80-associated radio-continuum emission detected with EMU is a roughly semi-circular feature with brighter emission in the western part (Fig. 1). It can be fitted by an ellipse with size  $2.7 \times 2.4$ , centred at RA(J2000)  $6^{\text{h}}30^{\text{m}}53.5^{\text{s}}$

**Table 1.** *Gaia* properties of stars within VdB-80. Columns [2] and [3] are FK5 (J2000) right ascension and declination positions. Column [4] is parallax and its associated error in milliarcseconds. Column [5] is distance and its associated error, as calculated from column [4], in parsecs. Column [6] is the right ascension proper motion, and column [7] is the declination proper motion in milliarcseconds per year.

[1]	[2]	[3]	[4]	[5]	[6]	[7]
Star name	RA (J2000) (h:m:s)	DEC (J2000) (d:m:s)	$\rho \pm \Delta\rho$ (mas)	$d \pm \Delta d$ (pc)	$\mu$ (RA) (mas yr <sup>-1</sup> )	$\mu$ (DEC) (mas yr <sup>-1</sup> )
HD 46060; NSV 2998; UCAC4 402-013688	06:30:49.8	-09:39:14.8	1.0711±0.0220	933±19	-3.526	0.154
BD-09 1497	06:30:48.3	-09:38:38.0	1.0532±0.0191	949±18	-3.428	0.226
UCAC4 402-013691	06:30:50.7	-09:39:26.1	1.0261±0.0184	975±18	-3.520	0.730
UCAC4 402-013693	06:30:51.0	-09:39:37.7	1.0430±0.0238	959±22	-3.190	0.270
Gaia DR3 3002950320576187904	06:30:49.8	-09:38:50.1	0.9483±0.0645	1055±72	-3.210	0.199

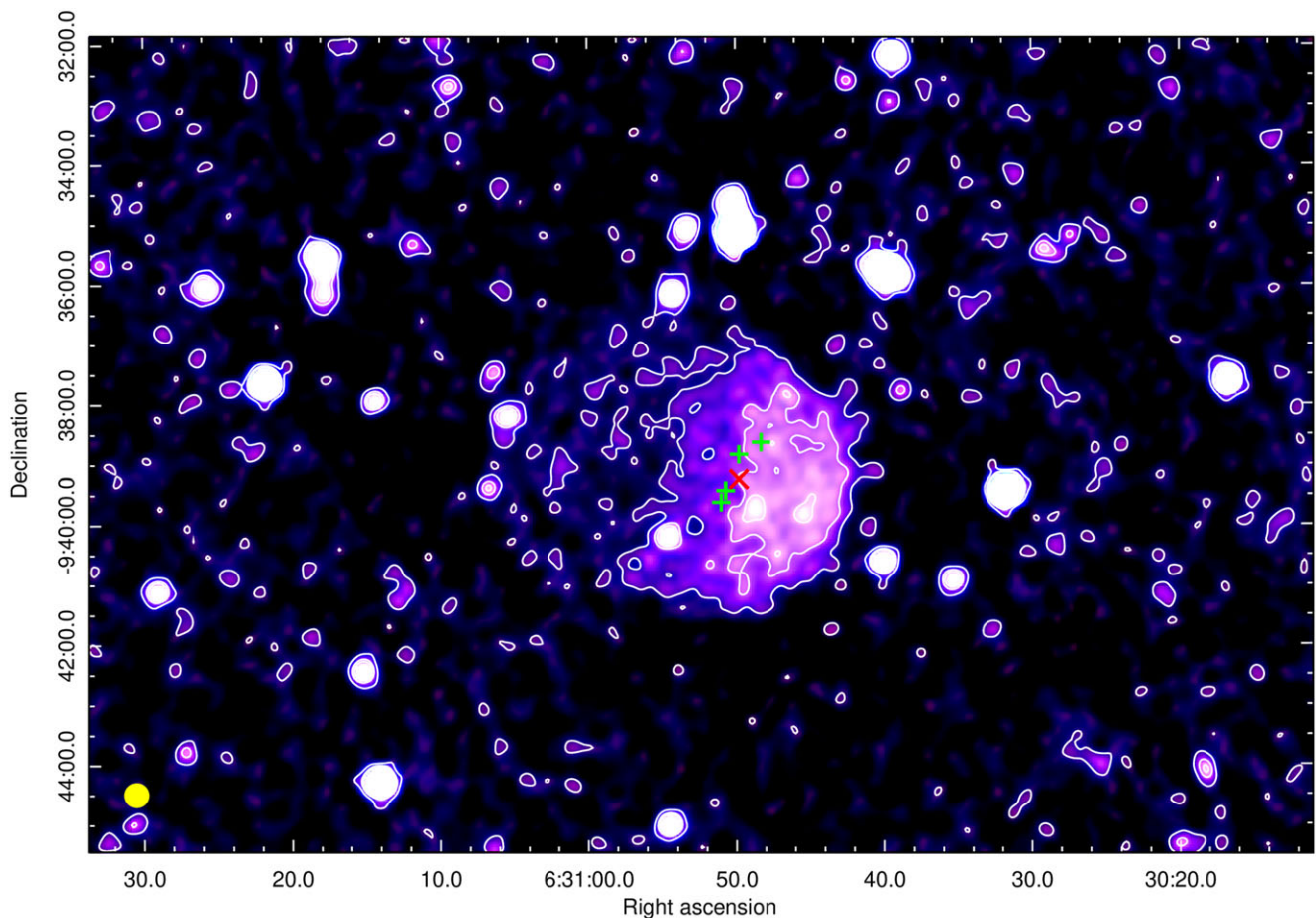


**Figure 1.** EMU radio-continuum image of Lagotis and VdB-80 at 944 MHz. Local RMS noise is  $20 \mu\text{Jy beam}^{-1}$ , and contours are at levels of 3, 10 and  $15\sigma$ . The image resolution is  $15 \times 15''$ , represented with the yellow circle in the bottom left corner. The red 'X' denotes the star HD 46060, and the green crosses denote the other stars in the cluster (see Table 1).

and Dec(J2000)  $9^{\circ}39'08''.6$ . The whole Lagotis structure has an integrated flux density of  $30.2 \pm 3.1 \text{ mJy}$ .<sup>b</sup> The western side of the feature appears much brighter than the eastern, with integrated flux densities of  $25.6 \pm 2.6 \text{ mJy}$  and  $4.6 \pm 0.5 \text{ mJy}$ .

<sup>b</sup>We measure the flux density and error following the same procedure as in Filipović et al. (2022) and Filipović et al. (2023).

Lagotis is detected in the NVSS survey at 1.4 GHz under the name NVSS 063048-094007 (Condon et al. 1998). Whilst this has been catalogued in NVSS, there has been no study regarding this emission as an HII region. The radio emission at 1.4 GHz has a measured flux of  $39.1 \pm 3.9 \text{ mJy}$ , and so a spectral index can be estimated, following the spectral index definition  $S \propto \nu^\alpha$  (Filipović & Tothill 2021b). Convolution of the EMU data to the same resolution

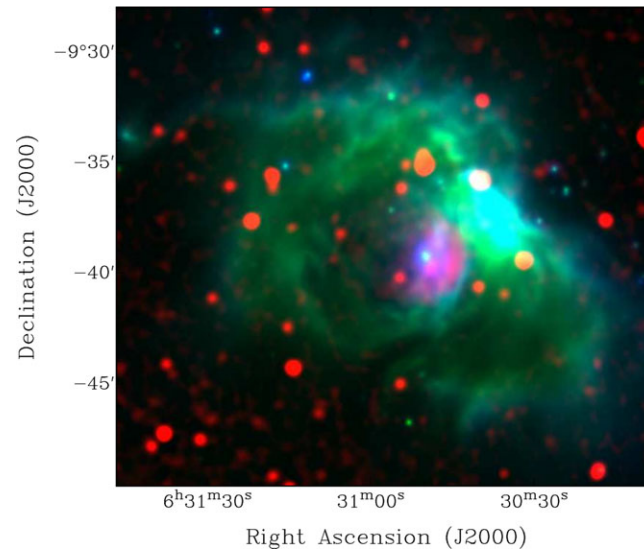


**Figure 2.** An RGB image tracing the near-infrared emission of VdB-80, where red is the EMU tile SB61077 (smoothed to a 25'' resolution) at 943.5 GHz, green is the WISE W3 band (12 $\mu$ m) and blue is the WISE W4 band (22 $\mu$ m).

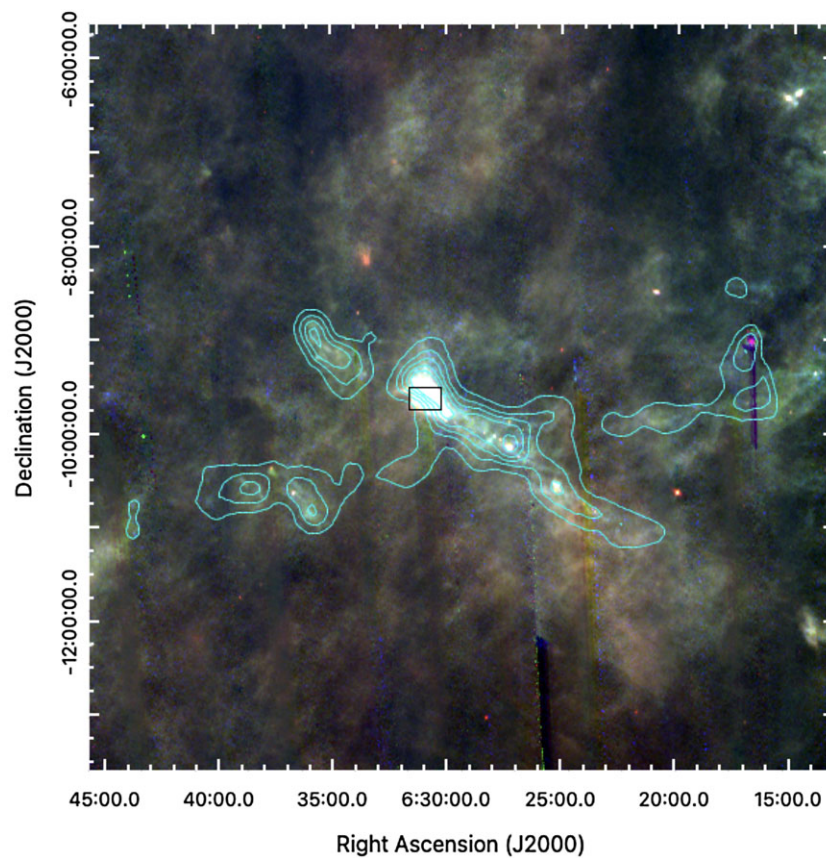


**Figure 3.** RGB composite image of the Crossbones filaments in far-infrared. Red is *AKARI* N160 (160  $\mu$ m band), green is *AKARI* WIDE-L (140  $\mu$ m band) and blue is *AKARI* WIDE-S (90  $\mu$ m band). Contours in cyan are generated from the  $^{12}\text{CO}$  ( $J = 1-0$ ) map provided by Ghosh *et al.* (2024). The black square in the image represents the size of Fig. 1, Lagotis corresponds to the bright emission in far-infrared. Fragmented vertical lines present in the image are artefacts from *AKARI* observations.

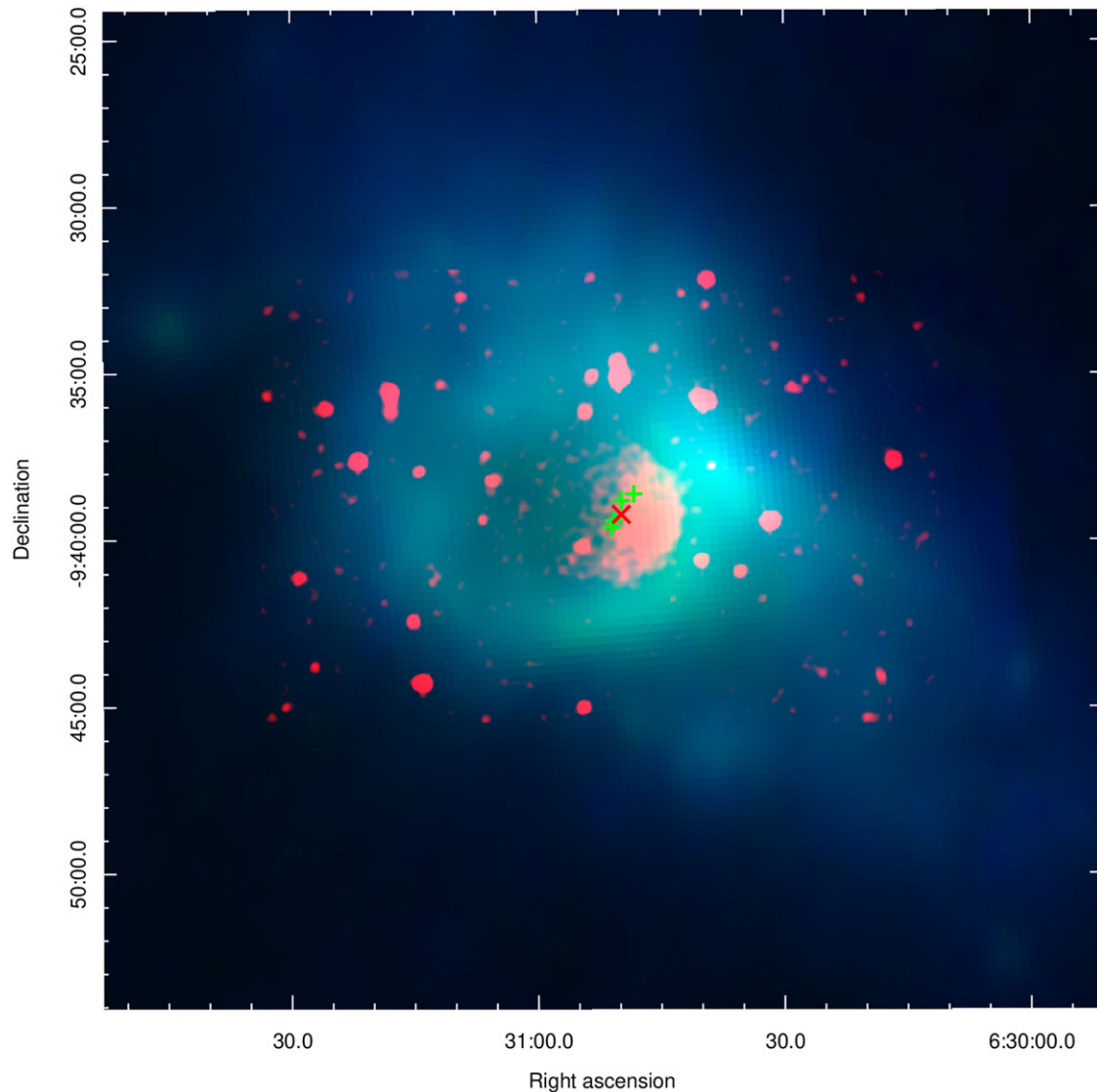


**Figure 4.** RGB image of Lagotis HII region and VdB-80, where red is the EMU radio image (943.5 MHz), green is an *AKARI* wide-S band (90  $\mu\text{m}$ ) image, and blue is an *AKARI* wide-L band (140  $\mu\text{m}$ ) image. The red 'X' denotes the star HD 46060, and the green crosses denote the other stars in the cluster (Table 1).

as NVSS (beam size =  $45 \times 45''$ , pixel size =  $10 \times 10''$ ) gives a spectral index of  $0.7 \pm 0.5$ , a fairly flat spectrum which is indicative of thermal radio emission. This spectral index estimate allows us to estimate a surface brightness value of  $\Sigma_{1\text{ GHz}} \sim 7.3 \times 10^{-22} \text{ W m}^{-2} \text{ Hz}^{-1} \text{ sr}^{-1}$ ; assuming a distance of 960 pc, this gives a luminosity at 1 GHz of  $\sim 3.6 \times 10^{12} \text{ W Hz}^{-1}$ . The approximately circular radio emission fits well inside the far-infrared emitting shell of gas and dust, as shown in Fig. 4.

### 3.2 Distance and size

*Gaia* parallaxes of the young stars associated with the RN VdB-80 and in the centre of the Lagotis HII region (Table 1) are taken from *Gaia* DR3 (Gaia Collaboration et al. 2016, 2023). The derived distances range from 914 to 1 127 pc. Since this range is much larger than the size of the stellar association,<sup>c</sup> we treat all stars as lying at

an error-weighted average distance of 960 pc, with an uncertainty of about 100 pc.

Wilson et al. (2005) estimated a distance to the Crossbones (and by extension Lagotis and VdB-80) of 465 pc using Hipparcos parallaxes, significantly closer than the distance we derive using *Gaia* data – this disparity is considered further in section 3.3. We take the value of  $960 \pm 100$  pc to be accurate as *Gaia* parallax is more reliable than the Hipparcos parallax used for the closer distance derivation (Al-Wardat et al. 2021).

Within the region of the radio-continuum emission, there are around 150 identified stars (Gaia Collaboration et al. 2016, 2023) with varying magnitudes and distances. The cluster of stars proposed to be associated with the VdB-80 RN includes 12 of these, of which we use a subset of five stars, including HD 46060 (Table 1); these appear to be central to the radio feature. These stars were chosen based on their central location in the radio-continuum feature, and within 40 arcsec of the proposed host star; HD 46060 (see Section 3.4.). The distance is taken to be the error-weighted

<sup>c</sup>The young stars spread over about an arcminute on the sky,  $< 1$  pc at  $\sim 1$  kpc.

**Table 2.** Near-IR 2MASS  $JHK_s$  magnitudes for the five star subset of the stellar cluster; and calculated near-IR colour excess ( $J - H/H - K_s$ ) and visual extinction  $A_V$ , derived according to Froebrich & del Burgo (2006). The error in extinction arises from the variation between  $J - H$  and  $H - K_s$  colours.

Star name	J	H	$K_s$	$J-H/H-K_s$	Extinction
HD 46060	8.153	8.134	8.105	0.65	$5.34 \pm 0.02$
BD-09 1497	9.643	9.490	9.378	1.60	$6.26 \pm 0.11$
UCAC4 402-013961	10.808	10.478	10.317	2.00	$6.96 \pm 0.20$
UCAC4 402-013693	10.395	10.297	10.239	1.69	$6.79 \pm 0.07$
Gaia DR3 3002950320576187904	13.702	12.867	12.532	2.50	$8.67 \pm 0.49$

average distance of the five stars, which puts VdB-80 at  $960 \pm 100$  pc. From the radio angular size of  $2.7 \times 2.4$ , we estimate the physical size to be  $0.75 \times 0.67 (\pm 0.09)$  pc.

2MASS extinction data show that the stellar cluster and VdB-80 are in the same plane and share a common distance. Table 2 shows near-IR 2MASS brightnesses for the same stars, along with colour excess ( $J - H/H - K_s$ ) and visual extinction  $A_V$ , calculated using formulae from Froebrich & del Burgo (2006) and Froebrich et al. (2007). The extinction values show a few magnitudes' reddening of the stars, similar to those found towards the Crossbones (Froebrich et al. 2007), indicating that they are embedded in the cloud. There is a distinct correlation between 2MASS extinction and *Gaia* distance (Tables 1 and 2): This suggests that HD 46060 is towards the front of the cloud (or may have cleared enough material to have lower extinction), while the other stars are more deeply embedded in the cloud behind HD 46060. The embedding of the stars underlines their association with the Crossbones cloud, and implies that the *Gaia* distance can be used for the cloud.

### 3.3 Crossbones

The 'Crossbones' in Monoceros is an 'X'-shaped molecular cloud structure prominent in both  $^{12}\text{CO}$  and  $^{13}\text{CO}$  maps (Maddalena et al. 1986; Kim et al. 2004). It was originally identified as part of the Orion-Monoceros cloud complex by Maddalena et al.: The Orion A and B clouds run approximately N-S, with northern and southern filaments running E-W. Crossbones appears to be part of the S filament, near where the Monoceros R2 (Mon R2) molecular cloud overlaps with the filament. At a distance of 800–900 pc Mon R2 lies far behind the Orion clouds (400–500 pc) and is not associated. Crossbones has been taken to be a spatially coherent structure because the velocities of its parts appear coherent. Maddalena et al., noting that the stars associated with VdB-80 had estimated distances  $\sim 800$  pc, suggested that the entire southern filament might be associated with Mon R2, rather than Orion. Wilson et al. (2005) derived a distance of  $\sim 460$  pc to the southern filament from *Hipparcos* stellar parallaxes.

The Lagotis HII region is embedded at the edge of the NE-SW arm of the Crossbones, close to the point where the arms cross (Fig. 3). This can be seen in the far-IR images, in which a larger far-IR bright region envelops the HII region, while the CO 1–0 emission has a cavity in the same place. The pressure of the HII region and the UV flux of its star are excavating the cavity in the molecular cloud, and the dust around the cavity is being heated up to generate the far-IR emission (Fig. 3). The calculated Lyman flux of HD 46060 (see Section 3.4.) is consistent with the HII region observed; this supports the argument that HD46060 and its neighbours not only illuminate VdB-80, but also power the Lagotis HII

region. Hence, the distance of these stars is the likely distance of this molecular gas structure.

The most likely interpretation of the data is that Crossbones is not a contiguous structure, but a superposition of a NE-SW filamentary cloud and the southern filament of the Orion-Monoceros cloud complex. The population of YSOs found by Lee & Chen (2009) towards Crossbones are largely found towards the NE-SW arm, which also appears brighter in CO and far-IR. We therefore suggest that the NE-SW arm of Crossbones is a dense star-forming cloud at the distance of (and possibly associated with) Mon R2; the SE-NW arm of Crossbones is simply part of the less dense southern Orion filament. The only evidence against this interpretation is the lack of velocity discontinuity between the two arms.

From the CO 1–0 data (Ghosh et al. 2024), we estimate an excitation temperature towards Lagotis of 12 K, compared to the 17 K found towards Mon R2 (Pokhrel et al. 2016). Considering the beam dilution in the rather large *Planck* beam, these temperature values are reasonably consistent.

### 3.4 The stellar cluster and the HII region

The *Gaia* proper motions of the main stars in the stellar cluster (Table 1) suggest that the cluster is moving into the Crossbones filaments near the centre (Fig. 3). Based on this movement, we give the HII region the designation 'Lagotis', as the stars are moving, or 'burrowing' into the HII region and the molecular cloud.<sup>d</sup>

In the larger scope of the stellar cluster, there is a large population of stars at a similar distance ( $\sim 1$  kpc); the majority of stars in this cluster have similar proper motion profiles to the Lagotis stars (Table 1). Due to its central location and brightness, we propose that HD 46060 is the main driver of the HII region. This star is the brightest in the central cluster and has generally been associated with the RN itself. The distance from HD 46060 to the edge of the bright emission is 0.49 pc, and we take this to be the radius of the HII region. We also assume the electron temperature of the HII region to be  $10^4$  K. Using the equations in Dyson & Williams (1997) and Schmiedeke et al. (2016), we derive an electron density of  $26 \text{ cm}^{-3}$ , which can then be used to estimate an ionising flux of  $10^{45.6} \text{ s}^{-1}$ .

HD 46060 has been variously classified as a spectral type of B8 (van den Bergh 1966; Ochsenbein 1980), B3ne (Racine 1968), B2 II (Houk & Swift 2000; Kharchenko 2001; Anderson & Francis 2012) and B2 III-IV (Aveni & Hunter 1972). Based on the most recent results, we adopt a spectral type of B2 II. HD 46060 is about  $4.5 \pm 1.5$  Myr old, (Ahumada et al. 2001), so its ionising flux is

<sup>d</sup>Lagotis comes from the Latin *Macrotis Lagotis*, the Australian Greater Bilby, <https://australian.museum/learn/animals/mammals/greater-bilby/>.

expected to be higher than the zero-age-main-sequence (ZAMS) value of  $10^{44.7} \text{ s}^{-1}$ . Panagia (1973) gives a range of ionising fluxes for B2 I-III that is consistent with our estimated ionising flux of  $10^{45.6} \text{ s}^{-1}$ .

We therefore put forward a self-consistent interpretation in which HD 46060 is a B2 II star with sufficient ionising flux to power the Lagotis HII region with radius 0.49 pc and electron density  $26 \text{ cm}^{-3}$ . This gives rise to thermal radio continuum emission, consistent with the estimated flux density.

Because VdB-80 sits on the edge of the cloud, there may be a champagne flow (Comeron 1997; Immer et al. 2014) from the Lagotis HII region that is not seen in the EMU image, with supersonic movement of ionised gas caused by a steep pressure and density gradient at the edge of the cloud (Bodenheimer, Tenorio-Tagle, & Yorke 1979). This is consistent with the roughly hemispherical shape of the HII region and may be the cause for the dim eastern side of the radio-continuum emission. More sensitive observations at additional frequencies may be able to test this possibility.

#### 4. Conclusion

Sensitive EMU observations have revealed radio-continuum emission at 943.5 MHz toward a known RN, VdB-80 (van den Bergh 1966). This is a unique feature for an object mainly known for its optical properties. The emission – nicknamed *Lagotis* – is measured to be  $30.2 \pm 0.3 \text{ mJy}$  and is comprised of bright (Western side) and dim (Eastern side) portions with flux densities of  $25.6 \pm 2.6$  and  $4.6 \pm 0.5 \text{ mJy}$ .

The radio-continuum detection is a circular feature with the brighter side pointed inward toward the Crossbones cloud filaments, accompanied by a bright shroud of far-infrared emission and an extended shell of mid-infrared emission (Figs. 2 and 4). This indicates heating of the cloud surrounding the RN, which is likely to be a byproduct of a HII region heating up the gas and dust surrounding its shell. This shows that the features associated with the RN and HII region extend much further than shown in visible wavelengths.

VdB-80 and Lagotis are situated at the edge of the Crossbones molecular cloud structure. We find the RN to be at a distance of  $960 \pm 100 \text{ pc}$  based on *Gaia* parallax values for a subset of stars in the stellar cluster association. From this distance, we estimate the size of the radio emission to be  $0.75 \times 0.67 (\pm 0.09 \text{ pc})$ , and we find that the Crossbones feature is most likely a superposition of two filamentary clouds associated with Orion (in the foreground) and Mon R2 (in the background).

The proper motion (Table 1) of the stellar cluster associated with the RN shows that the cluster is moving toward, and ‘into’ the cloud. The proposed driver of the HII region is HD 46060, a B2 II type star at the center of the stellar cluster, with enough ionising output to power the HII region, with an estimated electron density of  $26 \text{ cm}^{-3}$ . Irregularities in the radio feature as well as the far-infrared emitting shell may be generated from the other stars in the cluster with unknown spectral types.

Objects with low surface brightness, such as Lagotis, are becoming more prominent in high sensitivity surveys such as EMU. This discovery of the radio-continuum emission associated with an RN and its analysis has indicated that HD 46060 both powers Lagotis and illuminates VdB-80. ASKAP and other new-generation telescopes enable future observations and discoveries of RNe with radio-continuum emission.

**Acknowledgement.** This scientific work uses data obtained from Inyarrimanha Ilgari Bundara/the Murchison Radio-astronomy Observatory. We acknowledge the Wajarri Yamaji People as the Traditional Owners and native title holders of the Observatory site. CSIRO’s ASKAP radio telescope is part of the Australia Telescope National Facility (<https://ror.org/05qajvd42>). Operation of ASKAP is funded by the Australian Government with support from the National Collaborative Research Infrastructure Strategy. ASKAP uses the resources of the Pawsey Supercomputing Research Centre. Establishment of ASKAP, Inyarrimanha Ilgari Bundara, the CSIRO Murchison Radio-astronomy Observatory and the Pawsey Supercomputing Research Centre are initiatives of the Australian Government, with support from the Government of Western Australia and the Science and Industry Endowment Fund.

This work has made use of data from the European Space Agency (ESA) mission *Gaia* (<https://www.cosmos.esa.int/gaia>), processed by the *Gaia* Data Processing and Analysis Consortium (DPAC, <https://www.cosmos.esa.int/web/gaia/dpac/consortium>). Funding for the DPAC has been provided by national institutions, in particular the institutions participating in the *Gaia* Multilateral Agreement. This publication makes use of data products from the Two Micron All Sky Survey, which is a joint project of the University of Massachusetts and the Infrared Processing and Analysis Center/California Institute of Technology, funded by the National Aeronautics and Space Administration and the National Science Foundation. This research is based on observations with *AKARI*, a JAXA project with the participation of ESA.

**Data availability statement.** EMU data can be accessed through the CSIRO ASKAP Science Data Archive (CASDA) portal: <https://research.csiro.au/casda>. NVSS data can be obtained from the NVSS Postage Stamp Server: <https://www.cv.nrao.edu/nvss/postage.shtml>. All *Gaia* DR3 data are obtained from the *Gaia* Archive website: <https://gea.esac.esa.int/archive/>. Data from the 2MASS Point Source Catalogue are available from the NASA/IPAC Infrared Science Archive (IRSA): <https://irsa.ipac.caltech.edu/Missions/2mass.html>. WISE data is available from the NASA/IPAC Infrared Science Archive (IRSA): <https://irsa.ipac.caltech.edu/Missions/wise.html>. Data from the *AKARI* all-sky survey are available at the NASA/IPAC Infrared Science Archive (IRSA): <https://irsa.ipac.caltech.edu/data/AKARI/>.

**Funding statement.** MDF, GR, and SL acknowledge Australian Research Council (ARC) funding through grant DP200100784. DU acknowledges the financial support provided by the Ministry of Science, Technological Development, and Innovation of the Republic of Serbia through the contract 451-03-66/2024-03/200104 and for support through the joint project of the Serbian Academy of Sciences and Arts and Bulgarian Academy of Sciences ‘Optical search for Galactic and extragalactic supernova remnants’.

**Competing interests.** None.

#### References

- Ahumada, A. V., Clariá, J. J., Bica, E., Dutra, C. M., & Torres, M. C. 2001, *A&A*, **377**, 845
- Al-Wardat, M. A., Hussein, A. M., Al-Naimiy, H. M., & Barstow, M. A. 2021, *PASA*, **38**, e002
- Anderson, E., & Francis, C. 2012, *AstL*, **38**, 331
- Aveni, A. F., & Hunter, J. H. 1972, *AJ*, **77**, 17
- Bodenheimer, P., Tenorio-Tagle, G., & Yorke, H. W. 1979, *ApJ*, **233**, 85
- Bonatto, C., & Bica, E. 2009, *MNRAS*, **397**, 1915
- Burger-Scheidlin, C., et al. 2024, *A&A*, **684**, A150
- Comeron, F. 1997, *A&A*, **326**, 1195
- Condon, J. J., et al. 1998, *AJ*, **115**, 1693
- Dame, T. M., et al. 1987, *ApJ*, **322**, 706
- Doi, Y., et al. 2015, *PASJ*, **67**, 50
- Dyson, J. E., & Williams, D. A. 1997, *The physics of the Interstellar Medium* (Bristol, Philadelphia: Institute of Physics Pub), doi: [10.1201/9780585368115](https://doi.org/10.1201/9780585368115)

- Eiermann, J. M., Caputo, M., Lai, T. S. Y., & Witt, A. N. 2024, *MNRAS*, **529**, 1680
- Filipović, M. D., & Tothill, N. F. H. 2021a, *Multimessenger Astronomy in Practice*, doi: [10.1088/2514-3433/ac2256](https://doi.org/10.1088/2514-3433/ac2256)
- Filipović, M. D., & Tothill, N. F. H. 2021b, *Principles of Multimessenger Astronomy*, doi: [10.1088/2514-3433/ac087e](https://doi.org/10.1088/2514-3433/ac087e)
- Filipović, M. D., et al. 2022, *MNRAS*, **512**, 265
- Filipović, M. D., et al. 2023, *AJ*, **166**, 149
- Froebrich, D., & del Burgo, C. 2006, *MNRAS*, **369**, 1901
- Froebrich, D., Murphy, G. C., Smith, M. D., Walsh, J., & Del Burgo, C. 2007, *MNRAS*, **378**, 1447
- Gaia Collaboration, et al. 2016, *A&A*, **595**, A1
- Gaia Collaboration, et al. 2023, *A&A*, **674**, A1
- Ghosh, S., Remazeilles, M., & Delabrouille, J. 2024, *A&A*, **688**, A54
- Guzman, J., et al. 2019, *ASKAPsoft: ASKAP science data processor software*, *Astrophysics Source Code Library*, record ascl:1912.003
- Hotan, A. W., et al. 2021, *PASA*, **38**, e009
- Houk, N., & Swift, C. 2000, *VizieR Online Data Catalog: Michigan Catalogue of HD Stars*, Vol.5 (Houk+, 1999), *VizieR On-line Data Catalog: III/214*. Originally published in: Department of Astronomy, University of Michigan, Ann Arbor Michigan (1999)
- Immer, K., Cyganowski, C., Reid, M. J., & Menten, K. M. 2014, *A&A*, **563**, A39
- Khabibullin, I. I., Churazov, E. M., Bykov, A. M., Chugai, N. N., & Sunyaev, R. A. 2023, *MNRAS*, **521**, 5536
- Kharchenko, N. V. 2001, *Kinematika i Fizika Nebesnykh Tel*, **17**, 409
- Kim, B. G., Kawamura, A., Yonekura, Y., & Fukui, Y. 2004, *PASJ*, **56**, 313
- Kothes, R., Reich, P., Foster, T. J., & Reich, W. 2017, *A&A*, **597**, A116
- Lazarević, S., et al. 2024a, *RNAAS*, **8**, 107
- Lazarević, S., et al. 2024b, *PASA*, **41**, e032
- Lee, H.-T., & Chen, W. P. 2009, *ApJ*, **694**, 1423
- Maddalena, R. J., Morris, M., Moskowitz, J., & Thaddeus, P. 1986, *ApJ*, **303**, 375
- Magakian, T. Y. 2003, *A&A*, **399**, 141
- Mueller, K. E., & Graham, J. A. 2000, *PASP*, **112**, 1426
- Norris, R. P., et al. 2011, *PASA*, **28**, 215
- Norris, R. P., et al. 2021, *PASA*, **38**, e046
- Ochsenbein, F. 1980, *BICDS*, **19**, 74
- Orellana, R. B., De Biasi, M. S., Paz, L. G., Bustos Fierro, I. H., & Calderón, J. H. 2015, *New A*, **36**, 70
- Panagia, N. 1973, *AJ*, **78**, 929
- Pokhrel, R., et al. 2016, *MNRAS*, **461**, 22
- Racine, R. 1968, *ApJ*, **73**, 233
- Rozhkovskij, D. A., & Kurchakov, A. V. 1968, *TrAlm*, **11**, 3
- Sault, R. J., Teuben, P. J., & Wright, M. C. H. 1995, in *Astronomical Society of the Pacific Conference Series*, Vol. 77, *Astronomical Data Analysis Software and Systems IV*, ed. R. A. Shaw, H. E. Payne, & J. J. E. Hayes, 433
- Schmiedeke, A., et al. 2016, *A&A*, **588**, A143
- Sellgren, K. 1984, *ApJ*, **277**, 623
- Skrutskie, M. F., et al. 2006, *AJ*, **131**, 1163
- Smeaton, Z. J., et al. 2024, *RNAAS*, **8**, 158
- van den Bergh, S. 1966, *AJ*, **71**, 990
- Whitcomb, S. E., et al. 1981, *ApJ*, **246**, 416
- Wilson, B. A., Dame, T. M., Masheded, M. R. W., & Thaddeus, P. 2005, *A&A*, **430**, 523
- Wright, E. L., et al. 2010, *AJ*, **140**, 1868